A Reappraisal of Subtropical Subsurface Water Ice Stability on Mars

L. Lange, F. Forget, M. Vincendon, A. Spiga, E. Vos, O. Aharonson, E. Millour, A. Bierjon, R. Vandemeulebrouck

ADVANCING EARTH AND SPACE SCIENCES

Geophysical Research Letters

RESEARCH LETTER
10.1029/2023GL105177

A Reappraisal of Subtropical Subsurface Water Ice Stability on Mars

L. Lange[1], F. Forget[1], M. Vincendon[2], A. Spiga[1], E. Vos[1,3], O. Aharonson[3], E. Millour[1], A. Bierjon[1], and R. Vandemeulebrouck[1]

[1]Laboratoire de Météorologie Dynamique, Institut Pierre-Simon Laplace (LMD/IPSL), Sorbonne Université, Centre National de la Recherche Scientifique (CNRS), École Polytechnique, École Normale Supérieure (ENS), Paris, France, [2]Institut d'Astrophysique Spatiale, Université Paris-Saclay, CNRS, Orsay, France, [3]Department of Earth and Planetary Sciences, Weizmann Institute of Science, Rehovot, Israel

Key Points:

- We use a new model of steep slope microclimates to explore the stability of subsurface water ice on Mars at latitudes lower than 30°
- Our model shows that warm plains and large-scale atmospheric dynamics heat these slopes, preventing ice from being stable
- Subsurface ice is predicted to be present down to 30° of latitude, possibly down to 25° but for sparse slopes with favorable conditions

Supporting Information:

Supporting Information may be found in the online version of this article.

Correspondence to:

L. Lange,
lucas.lange@lmd.ipsl.fr

Citation:

Lange, L., Forget, F., Vincendon, M., Spiga, A., Vos, E., Aharonson, O., et al. (2023). A reappraisal of subtropical subsurface water ice stability on Mars. *Geophysical Research Letters*, *50*, e2023GL105177. https://doi.org/10.1029/2023GL105177

Received 28 JUN 2023
Accepted 31 AUG 2023

Abstract

Massive reservoirs of subsurface water ice in equilibrium with atmospheric water vapor are found poleward of 45° latitude on Mars. The absence of CO_2 frost on steep pole-facing slopes and simulations of atmospheric-soil water exchanges suggested that water ice could be stable underneath these slopes down to 25° latitude. We revisit these arguments with a new slope microclimate model. Our model shows that below 30° latitude, slopes are warmer than previously estimated as the air above is heated by warm surrounding plains. This additional heat prevents the formation of surface CO_2 frost and subsurface water ice for most slopes. Our model suggests the presence of subsurface water ice beneath pole-facing slopes down to 30° latitude, and possibly 25° latitude on sparse steep dusty slopes. While unstable ice deposits might be present, our results suggest that water ice is rarer than previously thought in the ±30° latitude range considered for human exploration.

Plain Language Summary

The presence of water ice near the equator is a key issue for future human exploration of Mars. In the current climate, this ice cannot exist near the equator but could be stable at accessible depths below pole-facing slopes down to latitudes of 25°, that is, close enough to the equator for a crewed mission. Here, we study the possible presence of this subsurface ice with a new model that simulates the microclimates associated with slopes on Mars. Our results show that, contrary to the arguments put forward in the literature, the slopes close to the equator (20°–30°) may in fact be too warm to allow subsurface water ice to be stable, and that the observations that suggested the presence of ice under these slopes can be explained otherwise by our model. Thus, the widespread presence of water ice under these slopes at subtropical latitudes is not demonstrated. However, our model cannot rule out the presence of ancient ice reservoirs, that would be slowly sublimating today.

1. Introduction

The Martian global water inventory is distributed in five reservoirs: the atmosphere, the surface ice, adsorbed water, hydrated minerals, and subsurface ice. The global average water content of the atmosphere, controlled by the sublimation of the northern polar cap, is about 10 pr-μm (expressed as precipitable microns of total column abundance) (M. D. Smith, 2002), while the perennial polar deposits represent 2/3 of the global exchangeable water inventory (nearly 3.2–4.7 × 10^6 km^3 of water for both caps, Montmessin et al., 2017). Depending on the regolith properties, the adsorbed water content can be up to 100 pr-μm (Montmessin et al., 2017). The Mars Odyssey Neutron Spectrometer (Boynton et al., 2004) and Fine-Resolution Epithermal Neutron Detector (Mitrofanov et al., 2018) revealed a significant amount of water in the shallow subsurface (≲1 m depth) at high latitudes (Boynton et al., 2002; Feldman et al., 2002; Malakhov et al., 2020). The total amount of water in this reservoir is poorly constrained because its bottom depth is not known. However, computations suggested that the upper meter of high-latitude regolith could contain nearly 10^4 more water than the atmosphere (Montmessin et al., 2017). Finally, hydrated minerals could contain up to 5 times the water content of all other water reservoirs combined (Wernicke & Jakosky, 2021).

Subsurface water ice (hereinafter referred to as subsurface ice) is of significant interest for the understanding and exploration of Mars. First, it affects the seasonal condensation and sublimation of polar caps, and thus directly impacts the CO_2 cycle (Haberle et al., 2008): because ground ice has a large thermal inertia, it stores heat during summer and releases it during winter, reducing the condensation rate of CO_2 ice. Second, this ice can record the history of volatile transport across water reservoirs (Vos et al., 2022). Finally, subsurface ice represents a major exploitable resource for future crewed exploration, as part of a strategy to rely on in-situ resources (Morgan et al., 2021). Thermal requirements for future crewed missions limit the possible landing site to latitudes lower than 30° (Grant et al., 2018; Morgan et al., 2021). The Mars Odyssey Neutron Spectrometer (MONS) has not observed ice enrichment in the first meter at such low latitudes (Diez et al., 2008), even if a recent impact revealed shallow subsurface ice down to 35°N latitude, which is the closest detection to the equator to date (Dundas et al., 2023). The existence and characterization of ice at low latitudes are therefore a significant challenge today (Bramson et al., 2021; Putzig et al., 2023).

As favorable landing conditions are frequently located at latitudes lower than 30°, we focus here on an assessment of subsurface ice stability within a 20°–30° latitude band. We will notably assess the stability of ice between 25° and 30°, a latitude range that will be referred to as "*subtropical latitudes*" in the following part of the paper. At such latitudes, subsurface ice is not expected to be stable on flat terrains (Schorghofer & Aharonson, 2005) but could be stable on pole-facing slopes which have cold microclimates. Two types of studies have suggested the presence of ice at subtropical latitudes under pole-facing terrains:

1. Vincendon et al. (2010a) studied the stability of CO_2 ice on pole-facing slopes at mid and subtropical latitudes in the Southern hemisphere. Seasonal CO_2 ice was not observed on slopes for latitudes lower than 34° while 1D thermal modeling indicated that ice should be present. They showed that the most likely explanation for the absence of frost at these latitudes lower than 34°, and the narrow distribution of CO_2 ice observations between 45° and 34°, was the presence of a latitude-dependent high thermal inertia material (most likely buried water ice with a latitude-dependent depth) under these slopes, which released heat during the winter and made the CO_2 ice unstable.
2. Numerical models by Aharonson and Schorghofer (2006) and Mellon and Sizemore (2022) of subsurface ice stability showed that ground ice could be stable with respect to diffusion down to 25° of latitude on steep pole-facing slopes.

Here, we show that subsurface ice is probably not stable on pole-facing slopes at latitudes lower than 30°, except in sparse locations with very favorable conditions and down to 25° latitude only (high slope angle, low thermal inertia, and high albedo). The model that is used to simulate slope microclimates and the subsurface ice stability is presented in Section 2. Using this new model, we show in Section 3.1 that the absence of CO_2 ice on low latitude slopes can be explained without requiring the presence of subsurface ice. We then apply our subsurface ice model to compute the theoretical water ice stability in Section 3.2 and show that previous studies may have overestimated the latitudinal extent of stable subsurface ice. The possible presence of subsurface ice in sparse favorable locations is discussed in Section 4. Conclusions are drawn in Section 5.

2. Methods and Model

2.1. Mars Planetary Climate Model

The current study uses the Mars Planetary Climate Model (PCM) version 6 (Forget et al., 1999, 2022). We have added a sub-grid slope parameterization to simulate slope microclimates. This parametrization is detailed and compared to observations in a companion paper (Lange et al., 2023a) that is summarized in Text S1 and illustrated in Figure S1 in Supporting Information S1. In short: for each PCM mesh, we decompose the cell as a distribution of sloped terrains (defined by characteristic slopes) and a flat terrain. On each sub-grid terrain, we compute the radiative transfer following Spiga et al. (2011), turbulent exchanges (Forget et al., 1999), and the condensation of volatiles (Forget et al., 1998; Navarro et al., 2014). The portion of the atmosphere above the ground within the cell is in equilibrium with a weighted average of these surface microclimates. Surface properties (albedo, emissivity, thermal inertia) are set to the observations from the Thermal Emission Spectrometer (TES, Christensen et al., 2001; Putzig & Mellon, 2007). A nominal dust opacity scenario is used (Montabone et al., 2015).

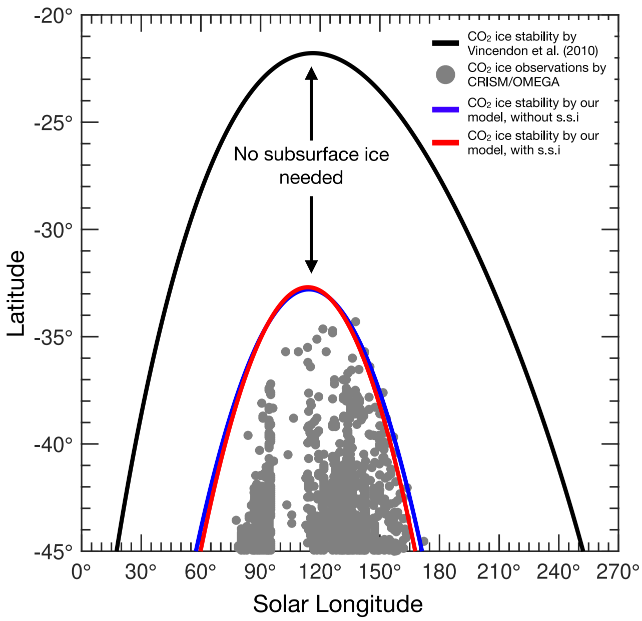

Figure 1. CO_2 ice stability on 30° pole-facing slopes in the Southern hemisphere as a function of the solar longitude (L_s, the Mars-Sun angle, measured from the Northern Hemisphere spring equinox where $L_s = 0°$). The black curve corresponds to the stability predicted by the 1D model of Vincendon et al. (2010a) with standard parameters and without subsurface ice; the blue curve represents the stability predicted by our 3D model without including subsurface ice; and the red curve represents the stability predicted by the model including subsurface ice as described in Section 3.2. CO_2 ice deposits observed on pole-facing slopes by Compact Reconnaissance Imaging Spectrometer for Mars (CRISM)/Observatoire pour la Minéralogie, l'Eau, les Glaces et l'Activité (OMEGA) (Vincendon, 2015; Vincendon et al., 2010a) are presented in gray dots.

2.2. Subsurface Ice Model

The model used to compute the ice table depth at equilibrium follows the approach of Aharonson and Schorghofer (2006), Mellon and Sizemore (2022), and Schorghofer and Aharonson (2005): subsurface ice is stable at a depth z if:

$$\overline{\left(\frac{p_{\text{vap,surf}}}{T_{\text{surf}}}\right)} \geq \overline{\left(\frac{p_{\text{sv}}(T_{\text{soil}}(z))}{T_{\text{soil}}(z)}\right)} \tag{1}$$

where overbars indicate time-averages over a complete Martian year, $p_{\text{vap, surf}}$ (Pa) is the vapor pressure at the surface, T_{surf} (K) is the surface temperature, $p_{\text{sv, soil}}$ (Pa) is the saturation vapor pressure which is a function of the soil temperature T_{soil} (K) (Murphy & Koop, 2005). $p_{\text{vap, surf}}$ is computed by the PCM, whose water cycle has been fully validated (Naar et al., 2021; Navarro et al., 2014) as well as near-surface vapor content through comparison with Phoenix measurements (Fischer et al., 2019). In this model, we also include the effect of surface water frost that stabilizes the ice table (Hagedorn et al., 2007; McKay, 2009; Williams et al., 2015). When ice is stable at depth z_{ice}, we set the thermal inertia of this layer and those below to 1,600 J m^{-2} K^{-1} $s^{-1/2}$, a mid-value between completely pore-filled ice and massive pure ice (Schorghofer & Aharonson, 2005; Siegler et al., 2012). This model is run for tens of years until the ice table depth has reached an equilibrium.

3. Results

3.1. CO_2 Ice Stability on Subtropical Slopes

We first demonstrate with our new model that the absence of CO_2 frost on subtropical pole-facing slopes can be explained without the presence of subsurface ice at these latitudes. In Vincendon et al. (2010a), the authors used a 1D version of the Mars PCM (without the sub-grid slope parameterization) to study the stability of CO_2 frost on 30° pole-facing slopes. The 1D PCM uses the same physics as the 3D model, but in the 1D, the atmosphere is in radiative equilibrium with the surface studied, and large-scale influence on the local meteorology are not considered. Following Vincendon et al. (2010a), CO_2 ice is stable and should be detected by Compact Reconnaissance Imaging Spectrometer for Mars (CRISM)/Observatoire pour la Minéralogie, l'Eau, les Glaces et l'Activité (OMEGA) at a given latitude if the CO_2 ice thickness predicted on the slope by the PCM exceeds hundreds of μm. Their predicted stability diagram of CO_2 frost on steep pole-facing slopes in Eastern Hellas (130–160°E) is presented in Figure 1. CO_2 frost observations by OMEGA and CRISM on pole-facing slopes reported in Vincendon (2015) and Vincendon et al. (2010a) are also plotted. Vincendon et al. (2010a) showed that the strong discrepancy between the theoretical stability and the observations, and notably the absence of frost between 22°S and 34°S could not be completely explained by varying the ice optical properties, dust opacity, or realistic surface thermal inertia. However, following Haberle et al. (2008), they suggested that the most likely explanation for this absence of frost was the presence of buried water ice under these slopes which released heat during the winter and made the CO_2 ice unstable. This conclusion was supported by the fact that the observed latitude/solar longitude distribution of CO_2 ice between 34° and 45° latitude is narrow, which requires a latitude-dependent heat source, in agreement with the behavior of subsurface water ice with a latitude-dependent depth.

We extend their study by computing the theoretical stability of CO_2 ice on 30° pole-facing slopes using our 3D model that simulates the slope microclimates. The same location and the same criterion for CO_2 ice stability as in Vincendon et al. (2010a) are used. First, we experimented without including subsurface ice beneath these slopes. The comparison between the predicted stability from their model and ours is illustrated in Figure 1. In our model, CO_2 frost is never stable for latitudes between ∼22° and ∼33° (±3° to account for the grid resolution) contrary to Vincendon et al. (2010a). To understand why, we compared the surface temperatures of a 30° pole-facing slope at

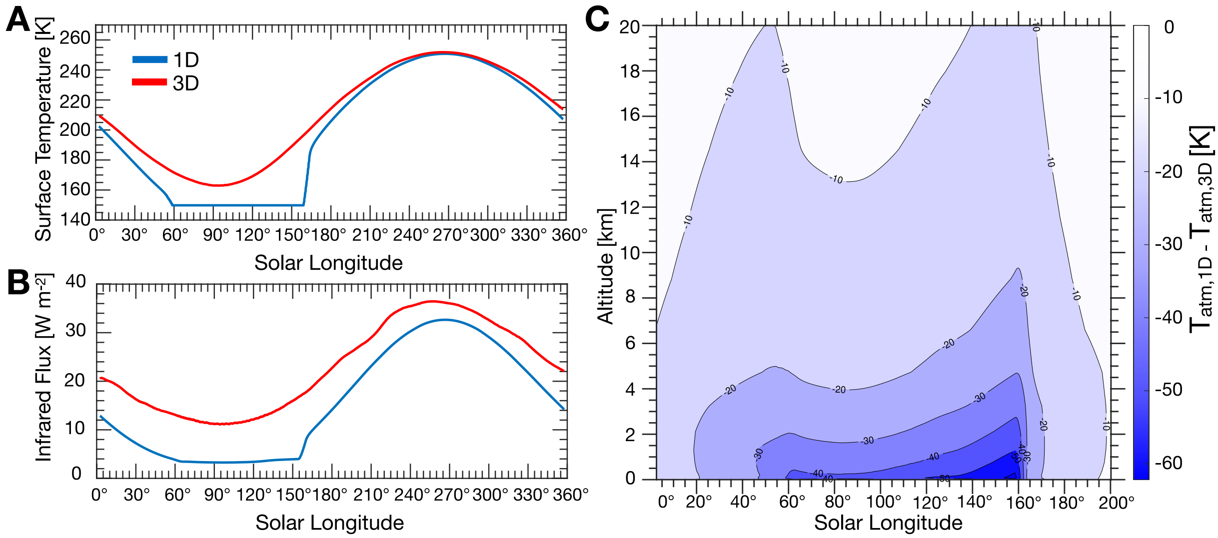

Figure 2. (a) Daily averaged surface temperature of a 30° pole-facing slope at 25°S during the year predicted by the 1D (red curve) and 3D (blue curve) model. (b) Same but for the downward infrared flux to the surface. (c) Difference of daily averaged atmospheric temperatures between the 1D and 3D models.

25°S computed by the 1D and 3D model (Figure 2a). In winter, the surface is 10–15 K warmer in the 3D model compared to the 1D model. We analyzed each of the terms appearing in the surface energy budget (Equation 1 from Text S1 in Supporting Information S1) and found that the major difference between the 1D and the 3D model is in the calculation of the infrared flux (Figure 2b). The difference is of the order of 10–15 W m^{-2}, which is enough to increase the temperature of a shaded slope by about 10° over most of winter and spring. Indeed, for these surfaces, the solar irradiance around the winter solstice is very low, and the surface temperature becomes very sensitive to the infrared flux.

Two differences explain this discrepancy:

1. In the 1D model, the atmosphere is in radiative equilibrium with the studied surface. Above a shaded slope, the atmosphere will be significantly colder than above a flat surface at the same coordinate, even if the slope is very small. In 3D, the atmosphere sees an average of sloped and flat sub-grid surfaces (weighted by the portion of the grid occupied by these slopes). Steep-sloped terrains actually represent a small percentage of the overall surface of Mars and are of limited length (tens or hundreds of meters, Aharonson & Schorghofer, 2006). Hence, the atmosphere is mostly in equilibrium with the warmer flat sub-grid surface and the slope microclimates do not significantly impact the state of the emitting atmosphere. Therefore, the air above the cold sloped surfaces is warmer in the 3D model compared to the 1D as it is heated by the nearby warm plains. A comparison of the state of the atmosphere between the 1D model with a 30° pole-facing slope and our 3D model at the same location is shown in Figure 2c. The difference in the air temperature near the surface (up to ~20–30 km) can be up to 30 or 40 K. This discrepancy is associated with a difference in the infrared flux of the order of 10 W m^{-2}, that is, what is observed in Figure 2b. While in our model, all sub-grid surfaces share the same atmosphere, actually, for a cold slope, the near-surface atmosphere may tend to cool (or warm) over the first 500 m through radiative exchanges with the surface, and then by convection over the first few kilometers (Read et al., 2017). Hence, the near-surface atmospheric temperature may be colder over a poleward-facing slope than over a flat area. However, the infrared emission by the atmosphere comes mainly from altitudes between 2 and 10 km (Figure 2 in Dufresne et al., 2005). At these altitudes, the atmosphere is not influenced by small slopes (less than 1 km in height difference, as observed on craters where frost is observed, Vincendon et al., 2010a, 2010b) because it is mixed by winds at altitudes that do not see these small reliefs. For these terrains, the approximation of a shared atmosphere for the calculation of the infrared flux is therefore more relevant.
2. The 1D model does not consider the possible contribution from large-scale meteorology. For example, during winter, the subsidence from the Hadley cell at mid and subtropical latitudes leads to an adiabatic heating of the atmosphere (Read et al., 2017, Figure S2 in Supporting Information S1). This warmer atmosphere increases

the infrared flux. We quantified this effect by computing the difference of infrared flux reaching a flat surface both in the 1D and 3D model at 25°S. The computation leads to a difference of ∼3–4 W m^{-2}.

Finally, it should also be noted that a warm atmosphere above a cold slope needs first to be cooled off before condensing on this surface (Text S1 in Supporting Information S1). The extra heat brought by the atmosphere when cooled can nearly reach 2% of the latent heat, reducing the total mass of CO_2 condensing, and thus its stability during daytime. When adding these three effects in the 1D model, CO_2 frost is not expected below 32°S, as in the 3D model.

Figure 1 (blue curve) also highlights that our 3D model predicts a delayed condensation and an earlier sublimation than with the 1D model between 45° and 35° latitude. These effects are not due to the surface albedo/emissivity between the two models. We show in Text S2 in Supporting Information S1 that the relative time difference between CO_2 condensation and sublimation for the 1D and 3D model is related to the relative difference in infrared fluxes. This relative difference in fluxes is of a factor of ∼1/3 during the southern autumn, and 2/3 in the southern spring (Figure S3a in Supporting Information S1). These ratios are the same as those found for the relative difference in the timing of condensation/sublimation of CO_2 (Figure S3b in Supporting Information S1).

However, we observe that CO_2 condensation occurs later in the observations than predicted by our model without subsurface ice, and earlier for the sublimation. Additionally, the narrow distribution of CO_2 ice is not well reproduced by our model. This suggests the contribution of a latitude-dependent parameter up to 32°S (the most equatorial detection by Vincendon, 2015) which is most likely subsurface water ice as demonstrated in Vincendon et al. (2010a). Considering the resolution of our model, we conclude that above 30°S, subsurface ice is required to explain the narrow distribution of CO_2 ice, but is not necessary to explain the absence of CO_2 ice equatorward.

3.2. Theoretical Stability of Subsurface Ice Beneath Pole-Facing Slopes

We now investigate the possible stability of subsurface ice on subtropical slopes following the approach described in Section 2.2. First, we test our method by calculating the stability of water ice under flat terrain (Figure 3). Subsurface ice is stable according to our model poleward of 55°, with brief excursions to 50° in regions of high albedo and low thermal inertia. Overall, the simulated spatial distribution of ice is consistent with MONS measurements (Diez et al., 2008; Pathare et al., 2018) and surface ice exposures (Dundas et al., 2021). However, some differences exist (e.g., MONS predicts ice down to latitudes 40°N, 45°S at some longitudes, and some recent impact craters reveal subsurface ice (Dundas et al., 2021) where it is not predicted by our model). These differences are discussed in Section 4. In addition, the depths at which ice is stable are broadly consistent with those published in the literature (Chamberlain & Boynton, 2007; Diez et al., 2008; Mellon et al., 2004; Pathare et al., 2018; Piqueux et al., 2019; Schorghofer & Aharonson, 2005) (Figure S4 in Supporting Information S1). At the Phoenix landing site, ice is predicted to be stable at a depth of 9 cm, in good agreement with direct in situ observations which reveal a depth between 5 and 18 cm (P. H. Smith et al., 2009).

We then model the possible stability of ice underneath pole-facing terrain with a slope angle of 30°. The results are presented in Figure 3b. The distribution of stable ground-ice extends equatorward, with limits up to ±35°. Excursions to lower latitudes are located in areas of low thermal inertia and high albedo (e.g., East Hellas, East Tharsis) and do not extend below 30° of latitudes. Our model thus differs from those of Aharonson and Schorghofer (2006) and of Mellon and Sizemore (2022) which predicted stable ice down to 25° latitude.

Two main differences between their models and ours can explain our more limited latitudinal extent for subsurface ice. First, in Aharonson and Schorghofer (2006)'s model, the infrared flux is computed as 4% of the solar flux at noon. Haberle and Jakosky (1991) showed that approximating the infrared flux as 2% of the solar flux at noon resulted in an underestimation of the infrared flux. Our calculations show that even if one replaces the 2% by 4% as in Aharonson and Schorghofer (2006), the infrared flux is still underestimated by about 2–6 W m^{-2} at subtropical latitudes with low dust opacity, and up to tens of W m^{-2} for dusty periods. Mellon and Sizemore (2022)'s model is a priori less sensitive to this last effect since the infrared flux is computed with the atmospheric model of Pollack et al. (1990). Differences may occur since our model has improved the radiative treatment of dust and clouds (Madeleine et al., 2011, 2012), and directly takes into account the dust observations by Montabone et al. (2015). Finally, in Aharonson and Schorghofer (2006) and Mellon and Sizemore (2022)'s models, $p_{vap,surf}$ in Equation 1 is computed with surface humidity from column-integrated measurements by TES obtained during daytime (M. D. Smith, 2002) if the surface is not at saturation. In our model, $p_{vap,surf}$ is computed by the Mars PCM that

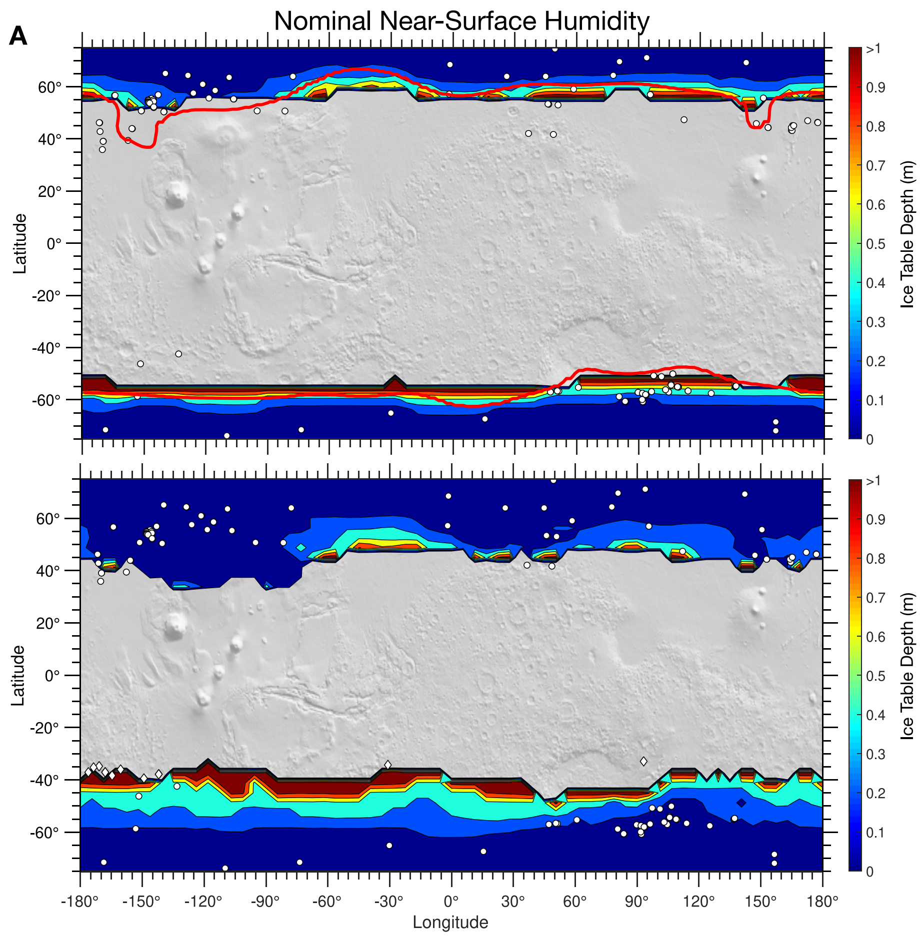

Figure 3. Theoretical stability of subsurface water-ice with respect to diffusion for (a) flat surfaces (b) 30° pole-facing slopes, using a nominal near-surface humidity. The red curve is the observed 10% Water-Equivalent Hydrogen contour, which is a good proxy for the presence of water ice in the shallow subsurface (Pathare et al., 2018). White dots indicate exposed water ice along cliff scarps and impact craters as reported in Dundas et al. (2021, 2023) White diamonds indicate exposed water ice along gullies (Khuller & Christensen, 2021).

solves the complete diurnal and seasonal water cycle and the vertical diffusion. Hence, as we are considering the complete diurnal cycle of water vapor (vs. daytime measurements for Aharonson and Schorghofer, 2006; Mellon and Sizemore, 2022), our surface humidity might be lower compared to the other models. Furthermore, the calculation of surface humidity from column-integrated measurements is complex because the vertical structure of the water vapor at the near-surface is not very constrained (Tamppari & Lemmon, 2020). To date, their models assume a well-mixed, hydrostatic, and isothermal atmosphere (Schorghofer & Aharonson, 2005). The difference between the predicted near-surface humidity from PCM and that obtained from TES daytime measurement interpolation can reach up to 0.05 Pa, that is, the humidity in Aharonson and Schorghofer (2006) and Mellon and Sizemore (2022) can be 20% higher than of the humidity retrieved with the PCM. Such a difference is significant for near-equatorial regions, where the stability of subsurface ice depends essentially on the near-surface water content (Song et al., 2023). Finally, we note that in Mellon and Sizemore (2022)'s model, the humidity used is 2.6 times that observed by TES, which tends to increase the stability of the near-equatorial ice in their model. This last point is discussed in Section 4.2.

4. Discussions

4.1. The Sparse Presence of Modeled Subsurface Water Ice Below ±30°N

Vincendon et al. (2010a) reported that water ice should be present within 1 m of the surface on all 20–30°pole-facing slopes down to about 25°S. They predicted that subsurface ice may be stable even at equatorward latitudes

(~20°S) with favorable slope conditions (very steep dusty slope). We investigate here the sensitivity of our model to the parameters used in this study. For instance, for very steep slopes (40°), our model suggests the presence of CO_2 ice down to 27°S. Even if these slopes are sparse (Aharonson & Schorghofer, 2006), no CO_2 ice detections have been made on such slopes at latitudes lower than 32°S (Vincendon, 2015; Vincendon et al., 2010a), suggesting the presence of water ice in these rare locations. Vincendon et al. (2010a) also showed the sensitivity of CO_2 ice formation/sublimation to surface properties. No clear constraints exist for the slope surface properties as some slopes exhibit low thermal inertia (Tebolt et al., 2020), favoring the condensation of CO_2; and some slopes reveal high-thermal inertia bedrock exposures (Edwards et al., 2009) which inhibit the formation of CO_2 frost. Yet, in the most favorable case (high albedo, low thermal inertia), our model suggests the presence of CO_2 ice down to 25°S where no ice is observed (Vincendon, 2015; Vincendon et al., 2010a). Hence, this suggests that water ice should be present beneath steep pole-facing slopes down to ±30° of latitudes on average, and could be present down to 25°S for sparse locations with favorable conditions (steep slopes ≥40°, high albedo, low thermal inertia).

Our model was validated by comparison with surface temperatures measured on sloped terrain and seasonal variations in water frost formation (Lange et al., 2023a). It turned out that our model could overestimate certain temperatures by 2 K on average, and up to 5 K on certain poleward-facing slopes, depending on local terrain properties (thermal inertia, slope angle, azimuth). If such a positive bias were confirmed, it could mean that ice stability would extend to 28° latitude for some 30° slopes (and 23° for some 40° slopes).

4.2. Possible Presence of Unstable Water Ice

The subsurface ice model used previously only allows us to determine the depth at which diffusion-formed subsurface water ice can be stable and in equilibrium with the atmosphere. According to our model, pore-filling water ice is stable down to latitudes of about 55° and locally 52°. However, MONS measurements (Diez et al., 2008; Pathare et al., 2018) have shown that water ice is expected underneath horizontal surfaces down to latitudes below 45° at Arcadia and Utopia Planitia, where our model does not predict stable ice (Figure 3). Seasonal variations in surface temperatures monitored by the Mars Climate Sounder also indicate traces of near-surface ice down to depths of less than 1 m at latitudes of 45° (Piqueux et al., 2019). Finally, ice excavations at impact craters show near-surface ice down to latitudes of 35°N (Byrne et al., 2009; Dundas et al., 2014, 2021, 2023). These exposed ice chunks may be more like pure ice than pore-filling due to the low regolith content in the ice (Dundas et al., 2014, 2021, 2023). In each case, our model, as well as those of Chamberlain and Boynton (2007), Mellon et al. (2004), and Schorghofer and Aharonson (2005) do not predict stable ice at these locations with current humidity (Figure 3).

To solve this paradox, Byrne et al. (2009), Chamberlain and Boynton (2007), and Mellon et al. (2004) doubled the humidity in their model to fit the MONS observations. Such a calculation assumes that the observed stable ice distribution is representative of that of the last several thousand years, where the authors assume the global average column abundance was at least twice as high as the 10 pr-μm observed today (M. D. Smith, 2002). Bramson et al. (2017) and Schorghofer and Forget (2012) proposed instead that these ices are traces of former ice formed as a result of past obliquity variations (e.g., Levrard et al., 2004; Madeleine et al., 2009, 2014), which are subsequently protected by the formation of a lag deposit. Thus, the subsurface ice observed today would not be in equilibrium with the surface and could act as a source of water vapor today (Schorghofer & Forget, 2012). Following Byrne et al. (2009), Chamberlain and Boynton (2007), and Mellon et al. (2004) approaches, we found that we needed to triple the near-surface humidity to find similar subsurface ice distribution (Figure S5a in Supporting Information S1). Note that in this extreme case, the average latitudinal extent of subsurface ice exceeds the average excess-ice limit observed by MONS.

The same question arises for the ice underneath pole-facing slopes where old unstable ice could persist. Possible direct observations of subsurface ice have been reported at 32.9°S (Khuller & Christensen, 2021) and geomorphic traces linked to the presence of ice in the subsurface have been detected down to latitudes of 30° (Viola & McEwen, 2018) whereas our model predicts stable subsurface ice down to latitudes of 35° at depths of the order of a meter. We test the sensitivity of this result to the surface humidity conditions by tripling the near-surface humidity for the flat terrains. The distribution obtained is presented in Figure S5b in Supporting Information S1. In this extreme scenario, subsurface ice is predicted to be stable down to ±30°N, with brief excursions down to ±25°N in favorable areas (high albedo, low thermal inertia). Hence, this experiment reinforces the conclusions drawn in Section 4.1, that is, that water ice could be present beneath steep pole-facing slopes down to ±30° of latitudes on average, and ±25° locally.

Our slope microclimate model without subsurface ice (Figure 1, blue curve) starts condensing CO_2 too early (by about 10° of L_s) compared to frost observations. By introducing subsurface ice at a depth given in Figure 3, we find that the new distribution for CO_2 frost stability differs only very slightly from that without subsurface ice (Figure 1, red curve). This result is expected because the ice is at depths greater than the thermal skin thickness associated with the seasonal cycle and thus does not have a strong impact on the surface energy budget. Hence, the narrow distribution of CO_2 ice observations for latitudes higher than 30°S requires subsurface ice with shallower latitude-dependent depths than those predicted by our model, as reported in Vincendon et al. (2010a). Even with the depths obtained from the triple humidity case, we can not correctly fit the narrow distribution, suggesting the presence of shallower (and thus unstable) ice. Future work will investigate the formation of glaciers during past epochs, the formation of lag deposits during their sublimation period, and their current preservation. Local measurements of seasonal variations of surface temperatures on sloped terrains could also help to constrain the presence of subsurface ice at low latitudes (e.g., Bandfield, 2007; Piqueux et al., 2019).

5. Conclusions

During this study, we have extended the work of Aharonson and Schorghofer (2006), Mellon and Sizemore (2022), and Vincendon et al. (2010a), who proposed the presence of subsurface water ice below 30° of latitude. On one hand, in Vincendon et al. (2010a), the absence of CO_2 frost on subtropical slopes was linked to the presence of high thermal inertia subsurface water ice that released heat during winter, preventing CO_2 condensation. Here, our model of slope microclimate shows that CO_2 ice is unstable on most slopes without subsurface water ice. Indeed, the plains surrounding the slope heat the atmosphere, increasing the infrared flux reaching the slope, warming the surface, and preventing it from reaching the CO_2 condensation temperature. On the other hand, the subsurface ice stability model from Aharonson and Schorghofer (2006) predicted stable ice down to 30° of latitude underneath pole-facing slopes, and down to 25° of latitude in dusty areas for the steepest slopes. Our subsurface ice stability model, coupled with the slope microclimate model, shows that slopes at these latitudes are too warm for stable subsurface ice with the current humidity and that this ground ice is only stable poleward of 30°. Our study reappraises this latitudinal extent of water ice proposed in these studies: subsurface water ice should be present beneath steep (≥30°) pole-facing slopes down to 30° of latitudes on average, with sparse excursions down to 25° for favorable locations (steep slopes, high albedo, low thermal inertia). However, subsurface stability models cannot conclude definitively about the presence of ice, since it does not model unstable ice remaining from past ice ages. Several markers suggest the possible presence of vestige unstable subsurface ice at low latitudes (Dundas et al., 2014, 2021; Viola & McEwen, 2018). Similarly, for latitudes above 32°S, our model does not exactly reproduce the narrow distribution of CO_2, suggesting the presence of shallower unstable ice. Modeling the accumulation, burial, and preservation of this ice during glacial periods, as well as more observational constraints on these near-equatorial slopes, will allow us to accurately characterize the presence or absence of subsurface ice. Our study suggests that water ice resources would be thus sparse at latitudes lower than 30°. Therefore, the accessibility of other water reservoirs like hydrated minerals should be more characterized at these latitudes as part of the strategy to rely on In Situ Resources for future crewed Martian missions.

Acknowledgments

This project has received funding from the European Research Council (ERC) under the European Union's Horizon 2020 research and innovation program (grant agreement 835275, project "Mars Through Time"). Mars PCM simulations were done thanks to the High-Performance Computing (HPC) resources of Centre Informatique National de l'Enseignement Supérieur (CINES) under the allocation n° A0100110391 made by Grand Equipement National de Calcul Intensif (GENCI). The authors thank Editor K. Lewis, M. Kreslavsky, and an anonymous reviewer for their comments. The authors thank N. Schörghofer, C. Dundas, and A. Khuller for insightful discussions.

Data Availability Statement

CO_2 frost detections by OMEGA and CRISM are from Vincendon (2015) and Vincendon et al. (2010a, 2010b). Data files for figures used in this analysis are available in a public repository, see Lange et al. (2023b). The Mars PCM used in this work can be downloaded with documentation from the SVN repository at https://svn.lmd.jussieu.fr/Planeto/trunk/LMDZ.MARS/. More information and documentation are available at https://www-planets.lmd.jussieu.fr.

References

Aharonson, O., & Schorghofer, N. (2006). Subsurface ice on Mars with rough topography. *Journal of Geophysical Research*, *111*(E11), E11007. https://doi.org/10.1029/2005JE002636

Bandfield, J. L. (2007). High-resolution subsurface water-ice distributions on Mars. *Nature*, *447*(7140), 64–67. https://doi.org/10.1038/nature05781

Boynton, W. V., Feldman, W., Mitrofanov, I., Evans, L., Reedy, R., Squyres, S., et al. (2004). The Mars Odyssey Gamma-Ray Spectrometer instrument suite. *Space Science Reviews*, *110*(1/2), 37–83. https://doi.org/10.1023/b:spac.0000021007.76126.15

Boynton, W. V., Feldman, W. C., Squyres, S. W., Prettyman, T. H., Bruckner, J., Evans, L. G., et al. (2002). Distribution of hydrogen in the near surface of Mars: Evidence for subsurface ice deposits. *Science*, *297*(5578), 81–85. https://doi.org/10.1126/science.1073722

Bramson, A., M. Andres, C., Bapst, J., Becerra, P., Courville, S. W., Dundas, C. M., et al. (2021). Mid-latitude ice on Mars: A science target for planetary climate histories and an exploration target for in situ resources. *Bulletin of the AAS*, *53*(4), 115. https://doi.org/10.3847/25c2cfeb.cc90422d

Bramson, A. M., Byrne, S., & Bapst, J. (2017). Preservation of midlatitude ice sheets on Mars. *Journal of Geophysical Research: Planets*, *122*(11), 2250–2266. https://doi.org/10.1002/2017je005357

Byrne, S., Dundas, C. M., Kennedy, M. R., Mellon, M. T., McEwen, A. S., Cull, S. C., et al. (2009). Distribution of mid-latitude ground ice on Mars from new impact craters. *Science*, *325*(5948), 1674–1676. https://doi.org/10.1126/science.1175307

Chamberlain, M. A., & Boynton, W. V. (2007). Response of Martian ground ice to orbit-induced climate change. *Journal of Geophysical Research*, *112*(E6), E06009. https://doi.org/10.1029/2006je002801

Christensen, P. R., Bandfield, J. L., Hamilton, V. E., Ruff, S. W., Kieffer, H. H., Titus, T. N., et al. (2001). Mars Global Surveyor Thermal Emission Spectrometer experiment: Investigation description and surface science results. *Journal of Geophysical Research*, *106*(E10), 23823–23871. https://doi.org/10.1029/2000je001370

Diez, B., Feldman, W., Maurice, S., Gasnault, O., Prettyman, T., Mellon, M., et al. (2008). H layering in the top meter of Mars. *Icarus*, *196*(2), 409–421. (Mars Polar Science IV). https://doi.org/10.1016/j.icarus.2008.02.006

Dufresne, J.-L., Fournier, R., Hourdin, C., & Hourdin, F. (2005). Net exchange reformulation of radiative transfer in the CO_2 15-μm band on Mars. *Journal of the Atmospheric Sciences*, *62*(9), 3303–3319. https://doi.org/10.1175/jas3537.1

Dundas, C. M., Byrne, S., McEwen, A. S., Mellon, M. T., Kennedy, M. R., Daubar, I. J., & Saper, L. (2014). HiRISE observations of new impact craters exposing Martian ground ice. *Journal of Geophysical Research: Planets*, *119*(1), 109–127. https://doi.org/10.1002/2013je004482

Dundas, C. M., Mellon, M. T., Conway, S. J., Daubar, I. J., Williams, K. E., Ojha, L., et al. (2021). Widespread exposures of extensive clean shallow ice in the midlatitudes of Mars. *Journal of Geophysical Research: Planets*, *126*(3), e2020JE006617. https://doi.org/10.1029/2020je006617

Dundas, C. M., Mellon, M. T., Posiolova, L. V., Miljković, K., Collins, G. S., Tornabene, L. L., et al. (2023). A Large new crater exposes the limits of water ice on Mars. *Geophysical Research Letters*, *50*(2), e2022GL100747. https://doi.org/10.1029/2022GL100747

Edwards, C. S., Bandfield, J. L., Christensen, P. R., & Fergason, R. L. (2009). Global distribution of bedrock exposures on Mars using THEMIS high-resolution thermal inertia. *Journal of Geophysical Research*, *114*(E11), E11001. https://doi.org/10.1029/2009JE003363

Feldman, W. C., Boynton, W. V., Tokar, R. L., Prettyman, T. H., Gasnault, O., Squyres, S. W., et al. (2002). Global distribution of neutrons from Mars: Results from Mars Odyssey. *Science*, *297*(5578), 75–78. https://doi.org/10.1126/science.1073541

Fischer, E., Martínez, G. M., Rennó, N. O., Tamppari, L. K., & Zent, A. P. (2019). Relative humidity on Mars: New results from the Phoenix TECP sensor. *Journal of Geophysical Research: Planets*, *124*(11), 2780–2792. https://doi.org/10.1029/2019JE006080

Forget, F., Hourdin, F., Fournier, R., Hourdin, C., Talagrand, O., Collins, M., et al. (1999). Improved general circulation models of the Martian atmosphere from the surface to above 80 km. *Journal of Geophysical Research*, *104*(E10), 24155–24175. https://doi.org/10.1029/1999JE001025

Forget, F., Hourdin, F., & Talagrand, O. (1998). CO_2 snowfall on Mars: Simulation with a general circulation model. *Icarus*, *131*(2), 302–316. https://doi.org/10.1006/icar.1997.5874

Forget, F., Millour, E., Bierjon, A., Delavois, A., Fan, S., Lange, L., et al. (2022). Challenges in Mars climate modelling with the LMD Mars global climate model, now called the Mars "Planetary Climate Model" (PCM). In *Seventh international workshop on the Mars atmosphere: Modelling and observations* (p. 1102).

Grant, J. A., Golombek, M. P., Wilson, S. A., Farley, K. A., Williford, K. H., & Chen, A. (2018). The science process for selecting the landing site for the 2020 Mars rover. *Planetary and Space Science*, *164*, 106–126. https://doi.org/10.1016/j.pss.2018.07.001

Haberle, R. M., Forget, F., Colaprete, A., Schaeffer, J., Boynton, W. V., Kelly, N. J., & Chamberlain, M. A. (2008). The effect of ground ice on the Martian seasonal CO_2 cycle. *Planetary and Space Science*, *56*(2), 251–255. https://doi.org/10.1016/j.pss.2007.08.006

Haberle, R. M., & Jakosky, B. M. (1991). Atmospheric effects on the remote determination of thermal inertia on Mars. *Icarus*, *90*(2), 187–204. https://doi.org/10.1016/0019-1035(91)90100-8

Hagedorn, B., Sletten, R. S., & Hallet, B. (2007). Sublimation and ice condensation in hyperarid soils: Modeling results using field data from Victoria Valley, Antarctica. *Journal of Geophysical Research*, *112*(F3), F03017. https://doi.org/10.1029/2006JF000580

Khuller, A., & Christensen, P. (2021). Evidence of exposed dusty water ice within Martian gullies. *Journal of Geophysical Research: Planets*, *126*(2), e2020JE006539. https://doi.org/10.1029/2020JE006539

Lange, L., Forget, F., Dupont, E., Vandemeulebrouck, R., Spiga, A., Millour, E., et al. (2023a). Modelling sub-grid scale slope microclimates in the Mars Planetary Climate Model. *Journal of Geophysical Research: Planets*. https://doi.org/10.1029/2023JE007915

Lange, L., Forget, F., Vincendon, M., Spiga, A., Vos, E., Aharonson, O., et al. (2023b). A reappraisal of subtropical subsurface water ice stability on Mars [Dataset]. Harvard Dataverse. https://doi.org/10.7910/DVN/NJXTTG

Levrard, B., Forget, F., Montmessin, F., & Laskar, J. (2004). Recent ice-rich deposits formed at high latitudes on Mars by sublimation of unstable equatorial ice during low obliquity. *Nature*, *431*(7012), 1072–1075. https://doi.org/10.1038/nature03055

Madeleine, J.-B., Forget, F., Head, J. W., Levrard, B., Montmessin, F., & Millour, E. (2009). Amazonian northern mid-latitude glaciation on Mars: A proposed climate scenario. *Icarus*, *203*(2), 390–405. https://doi.org/10.1016/j.icarus.2009.04.037

Madeleine, J.-B., Forget, F., Millour, E., Montabone, L., & Wolff, M. J. (2011). Revisiting the radiative impact of dust on Mars using the LMD Global Climate Model. *Journal of Geophysical Research*, *116*(E11), E11010. https://doi.org/10.1029/2011je003855

Madeleine, J.-B., Forget, F., Millour, E., Navarro, T., & Spiga, A. (2012). The influence of radiatively active water ice clouds on the Martian climate. *Geophysical Research Letters*, *39*(23), L23202. https://doi.org/10.1029/2012gl053564

Madeleine, J.-B., Head, J. W., Forget, F., Navarro, T., Millour, E., Spiga, A., et al. (2014). Recent ice ages on Mars: The role of radiatively active clouds and cloud microphysics. *Geophysical Research Letters*, *41*(14), 4873–4879. https://doi.org/10.1002/2014GL059861

Malakhov, A. V., Mitrofanov, I. G., Litvak, M. L., Sanin, A. B., Golovin, D. V., Djachkova, M. V., et al. (2020). Ice permafrost "oases" close to Martian equator: Planet neutron mapping based on data of FREND instrument onboard TGO orbiter of Russian-European ExoMars Mission. *Astronomy Letters*, *46*(6), 407–421. https://doi.org/10.1134/s1063773720060079

McKay, C. P. (2009). Snow recurrence sets the depth of dry permafrost at high elevations in the McMurdo Dry Valleys of Antarctica. *Antarctic Science*, *21*(1), 89–94. https://doi.org/10.1017/S0954102008001508

Mellon, M. T., Feldman, W. C., & Prettyman, T. H. (2004). The presence and stability of ground ice in the southern hemisphere of Mars. *Icarus*, *169*(2), 324–340. https://doi.org/10.1016/j.icarus.2003.10.022

Mellon, M. T., & Sizemore, H. G. (2022). The history of ground ice at Jezero Crater Mars and other past, present, and future landing sites. *Icarus*, *371*, 114667. https://doi.org/10.1016/j.icarus.2021.114667

Mitrofanov, I., Malakhov, A., Bakhtin, B., Golovin, D., Kozyrev, A., Litvak, M., et al. (2018). Fine resolution epithermal neutron detector (FREND) onboard the ExoMars trace gas orbiter. *Space Science Reviews*, *214*(5), 86. https://doi.org/10.1007/s11214-018-0522-5

Montabone, L., Forget, F., Millour, E., Wilson, R., Lewis, S., Cantor, B., et al. (2015). Eight-year climatology of dust optical depth on Mars. *Icarus*, *251*, 65–95. (Dynamic Mars). https://doi.org/10.1016/j.icarus.2014.12.034

Montmessin, F., Smith, M. D., Langevin, Y., Mellon, M. T., & Fedorova, A. (2017). The water cycle. In R. M. Haberle, R. T. Clancy, F. Forget, M. D. Smith, & R. W. Zurek (Eds.), *Asteroids, comets, meteors - ACM2017* (pp. 295–337). https://doi.org/10.1017/9781139060172.011

Morgan, G. A., Putzig, N. E., Perry, M. R., Sizemore, H. G., Bramson, A. M., Petersen, E. I., et al. (2021). Availability of subsurface water-ice resources in the northern mid-latitudes of Mars. *Nature Astronomy*, *5*(3), 230–236. https://doi.org/10.1038/s41550-020-01290-z

Murphy, D. M., & Koop, T. (2005). Review of the vapour pressures of ice and supercooled water for atmospheric applications. *Quarterly Journal of the Royal Meteorological Society*, *131*(608), 1539–1565. https://doi.org/10.1256/qj.04.94

Naar, J., Forget, F., Vals, M., Millour, E., Bierjon, A., González-Galindo, F., & Richard, B. (2021). Modeling the global water cycle on Mars with improved physical parametrization. In *European planetary science congress* (p. EPSC2021-559). https://doi.org/10.5194/epsc2021-559

Navarro, T., Madeleine, J.-B., Forget, F., Spiga, A., Millour, E., Montmessin, F., & Määttänen, A. (2014). Global climate modeling of the Martian water cycle with improved microphysics and radiatively active water ice clouds. *Journal of Geophysical Research: Planets*, *119*(7), 1479–1495. https://doi.org/10.1002/2013JE004550

Pathare, A. V., Feldman, W. C., Prettyman, T. H., & Maurice, S. (2018). Driven by excess? Climatic implications of new global mapping of near-surface water-equivalent hydrogen on Mars. *Icarus*, *301*, 97–116. https://doi.org/10.1016/j.icarus.2017.09.031

Piqueux, S., Buz, J., Edwards, C. S., Bandfield, J. L., Kleinböhl, A., Kass, D. M., & Hayne, P. O. (2019). Widespread shallow water ice on Mars at high latitudes and midlatitudes. *Geophysical Research Letters*, *46*(24), 14290–14298. https://doi.org/10.1029/2019gl083947

Pollack, J. B., Haberle, R. M., Schaeffer, J., & Lee, H. (1990). Simulations of the general circulation of the Martian atmosphere: 1. Polar processes. *Journal of Geophysical Research*, *95*(B2), 1447–1473. https://doi.org/10.1029/jb095ib02p01447

Putzig, N. E., & Mellon, M. T. (2007). Apparent thermal inertia and the surface heterogeneity of Mars. *Icarus*, *191*(1), 68–94. https://doi.org/10.1016/j.icarus.2007.05.013

Putzig, N. E., Morgan, G. A., Sizemore, H. G., Baker, D. M. H., Petersen, E. I., Pathare, A. V., et al. (2023). Ice resource mapping on Mars. In *Handbook of space resources* (pp. 583–616). Springer International Publishing. https://doi.org/10.1007/978-3-030-97913-3_16

Read, P. L., Galperin, B., Larsen, S. E., Lewis, S. R., Määttänen, A., Petrosyan, A., et al. (2017). The Martian planetary boundary layer. In *The atmosphere and climate of Mars* (pp. 172–202). Cambridge University Press. https://doi.org/10.1017/9781139060172.007

Schorghofer, N., & Aharonson, O. (2005). Stability and exchange of subsurface ice on Mars. *Journal of Geophysical Research*, *110*(E5), E05003. https://doi.org/10.1029/2004JE002350

Schorghofer, N., & Forget, F. (2012). History and anatomy of subsurface ice on Mars. *Icarus*, *220*(2), 1112–1120. https://doi.org/10.1016/j.icarus.2012.07.003

Siegler, M., Aharonson, O., Carey, E., Choukroun, M., Hudson, T., Schorghofer, N., & Xu, S. (2012). Measurements of thermal properties of icy Mars regolith analogs. *Journal of Geophysical Research*, *117*(E3), E03001. https://doi.org/10.1029/2011JE003938

Smith, M. D. (2002). The annual cycle of water vapor on Mars as observed by the Thermal Emission Spectrometer. *Journal of Geophysical Research*, *107*(E11), 25-1–25-19. https://doi.org/10.1029/2001JE001522

Smith, P. H., Tamppari, L. K., Arvidson, R. E., Bass, D., Blaney, D., Boynton, W. V., et al. (2009). H_2O at the Phoenix landing site. *Science*, *325*(5936), 58–61. https://doi.org/10.1126/science.1172339

Song, H., Zhang, J., Liu, Y., Sun, Y., & Ni, D. (2023). Modeling the distribution of subsurface seasonal water ice with varying atmospheric conditions at northern low to midlatitudes on Mars. *Icarus*, *389*, 115262. https://doi.org/10.1016/j.icarus.2022.115262

Spiga, A., Forget, F., Madeleine, J.-B., Montabone, L., Lewis, S. R., & Millour, E. (2011). The impact of Martian mesoscale winds on surface temperature and on the determination of thermal inertia. *Icarus*, *212*(2), 504–519. https://doi.org/10.1016/j.icarus.2011.02.001

Tamppari, L. K., & Lemmon, M. T. (2020). Near-surface atmospheric water vapor enhancement at the Mars Phoenix lander site. *Icarus*, *343*, 113624. https://doi.org/10.1016/j.icarus.2020.113624

Tebolt, M., Levy, J., Goudge, T., & Schorghofer, N. (2020). Slope, elevation, and thermal inertia trends of Martian recurring slope lineae initiation and termination points: Multiple possible processes occurring on coarse, sandy slopes. *Icarus*, *338*, 113536. https://doi.org/10.1016/j.icarus.2019.113536

Vincendon, M. (2015). Identification of Mars gully activity types associated with ice composition. *Journal of Geophysical Research: Planets*, *120*(11), 1859–1879. https://doi.org/10.1002/2015je004909

Vincendon, M., Forget, F., & Mustard, J. (2010b). Water ice at low to midlatitudes on Mars. *Journal of Geophysical Research*, *115*(E10), E10001. https://doi.org/10.1029/2010JE003584

Vincendon, M., Mustard, J., Forget, F., Kreslavsky, M., Spiga, A., Murchie, S., & Bibring, J.-P. (2010a). Near-tropical subsurface ice on Mars. *Geophysical Research Letters*, *37*(1), L01202. https://doi.org/10.1029/2009gl041426

Viola, D., & McEwen, A. S. (2018). Geomorphological evidence for shallow ice in the Southern Hemisphere of Mars. *Journal of Geophysical Research: Planets*, *123*(1), 262–277. https://doi.org/10.1002/2017je005366

Vos, E., Aharonson, O., Schörghofer, N., Forget, F., Millour, E., Rossi, L., et al. (2022). Stratigraphic and isotopic evolution of the Martian polar caps from paleo-climate models. *Journal of Geophysical Research: Planets*, *127*(3), e2021JE007115. https://doi.org/10.1029/2021je007115

Wernicke, L. J., & Jakosky, B. M. (2021). Martian hydrated minerals: A significant water sink. *Journal of Geophysical Research: Planets*, *126*(3), e2019JE006351. https://doi.org/10.1029/2019JE006351

Williams, K., McKay, C. P., & Heldmann, J. (2015). Modeling the effects of Martian surface frost on ice table depth. *Icarus*, *261*, 58–65. https://doi.org/10.1016/j.icarus.2015.08.005

References From the Supporting Information

Christensen, P. R., Jakosky, B. M., Kieffer, H. H., Malin, M. C., McSween, J., Harry, Y., et al. (2004). The Thermal Emission Imaging System (THEMIS) for the Mars 2001 Odyssey Mission. *Space Science Reviews*, *110*(1), 85–130. https://doi.org/10.1023/B:SPAC.0000021008.16305.94

de Vrese, P., Schulz, J.-P., & Hagemann, S. (2016). On the representation of heterogeneity in land-surface–atmosphere coupling. *Boundary-Layer Meteorology*, *160*(1), 157–183. https://doi.org/10.1007/s10546-016-0133-1

Pitman, A. J. (2003). The evolution of, and revolution in, land surface schemes designed for climate models. *International Journal of Climatology*, *23*(5), 479–510. https://doi.org/10.1002/joc.893

Spiga, A., & Forget, F. (2008). Fast and accurate estimation of solar irradiance on Martian slopes. *Geophysical Research Letters*, *35*(15), L15201. https://doi.org/10.1029/2008gl034956

Wang, F., Cheruy, F., & Dufresne, J. L. (2016). The improvement of soil thermodynamics and its effects on land surface meteorology in the IPSL climate model. *Geoscientific Model Development*, *9*(1), 363–381. https://doi.org/10.5194/gmd-9-363-2016